Published in final edited form as:
Anal Chem. 2011 February 15; 83(4): 1408–1417. doi:10.1021/ac102897h.

Rapid prototyping of arrayed microfluidic systems in polystyrene for cell-based assays

Edmond W.K. Young[1,*], **Erwin Berthier**[1,*], **David J. Guckenberger**[1], **Eric Sackmann**[1], **Casey Lamers**[2], **Ivar Meyvantsson**[2], **Anna Huttenlocher**[3], and **David J. Beebe**[1,#]

[1]Department of Biomedical Engineering, Wisconsin Institutes for Medical Research, University of Wisconsin-Madison, 1111 Highland Avenue, Madison, WI 53705

[2]Bellbrook Labs, 5500 Nobel Drive, Suite 250, Madison, WI 53711

[3]Department of Pediatrics, University of Wisconsin-Madison, 4205 Microbial Sciences Building, Madison, WI 53705

Abstract

Microfluidic cell-based systems have enabled the study of cellular phenomena with improved spatiotemporal control of the microenvironment and at increased throughput. While PDMS has emerged as the most popular material in microfluidics research, it has specific limitations that prevent microfluidic platforms from achieving their full potential. We present here a complete process, ranging from mold design to embossing and bonding, that describes the fabrication of polystyrene (PS) microfluidic devices with similar cost and time expenditures as PDMS-based devices. Emphasis was placed on creating methods that can compete with PDMS fabrication methods in terms of robustness, complexity and time requirements. To achieve this goal several improvements were made to remove critical bottlenecks in existing PS embossing methods. First, traditional lithography techniques were adapted to fabricate bulk epoxy molds capable of resisting high temperatures and pressures. Second, a method was developed to emboss through-holes in a PS layer, enabling creation of large arrays of independent microfluidic systems on a single device without need to manually create access ports. Third, thermal bonding of PS layers was optimized in order to achieve quality bonding over large arrays of microsystems. The choice of materials and methods were validated for biological function using two different cell-based applications to demonstrate the versatility of our streamlined fabrication process.

Introduction

The major advances in microfluidics and recent progress in bioMEMS can be largely attributed to the emergence of soft lithography as a fast, facile, and cost-effective method for microfabrication.[1,2] The ability to exploit the properties of elastomeric materials such as poly(dimethylsiloxane) (PDMS) for rapid prototyping of microscale systems has allowed scientists and engineers to employ iterative design processes to efficiently optimize microchannel configurations for diverse applications and across various disciplines (Figure 1).[3–8] The simplicity and accessibility of soft lithography has also enabled a unique design methodology that is both precise and versatile, facilitating novel and creative experimental approaches to current problems in biology. The popularity of PDMS is due not only to its convenient fabrication process, but also to a number of attractive physical and mechanical

[#]To whom corresponding may be addressed: Wisconsin Institutes for Medical Research, 1111 Highland Avenue, Room 6009, Madison, WI, USA, 53705, Tel: 1-608-262-2260, djbeebe@wisc.edu.
[*]Authors contributed equally

properties (e.g., optical transparency, permeability, and pliability) that have proven useful for various cell-based applications, ranging from the compartmentalization of cocultured cell types in complex geometries to the application of controlled mechanical and chemical stimuli on cells.[9–19]

While these advances have established PDMS as an important material for enabling novel experimental methods that are not achievable with conventional platforms, various studies have also demonstrated that PDMS has adverse effects in cell-based studies. PDMS has been shown to recover its hydrophobicity upon surface treatments,[20] absorb small hydrophobic molecules,21 leach uncrosslinked oligomers into solution,22 and allow evaporation through the bulk material.23 Such effects demonstrate that PDMS can actively alter the biochemical microenvironment in which cells are cultured, which importantly can create biases in biological conclusions that are distinct from other biases (e.g., substrate stiffness25) inherent in *in vitro* experimentation.22,24 In addition, the adoption of PDMS-based microfluidic platforms in the biology research community has been hindered by several contributing factors, namely (1) lack of characterization of PDMS for biological applications; (2) challenges associated with corroborating PDMS-based results with results from conventional platforms;26,27 and (3) scarcity of microfluidic platforms conforming to standardized formats. Efforts to improve integration of microfluidics into biology laboratories, such as use of passive pumping for automated liquid handling28,29 and design of arrayed devices compatible with plate-readers,30–32 have begun to acknowledge the importance of conforming to existing infrastructure and technology. However, to promote further integration of microfluidic technologies into biology laboratories, we must continue to address concerns associated with PDMS, and design systems that carefully consider the needs of biologists.[33]

From the biologist's perspective, the most commonly used material for in vitro cell-based research is polystyrene (PS), due to its commercial availability in tissue culture plasticware. Because PS has become central to mammalian cell culture research, and therefore is unlikely to be supplanted in popularity by other materials, making PS-based microfluidic devices more readily available can potentially reduce the barriers that hinder widespread adoption of microfluidic technologies. Moreover, PS is amenable to mass manufacturing processes that facilitate translation of microscale systems from simple laboratory tools to commercially marketable products, further expanding its potential impact in biological research. This trend is highlighted by emergence of various companies offering specific plastic microfluidic cell-based assays (e.g., Bellbrook Labs, Madison, WI, USA; ibidi, Munich, Germany).

To date, thermoplastic materials have been used in a relatively small proportion of published work in microfluidics compared to PDMS.34,35 Of this work, the main choices of thermoplastic material for microfabrication include poly(methylmethacrylate) (PMMA),36–38 polycarbonate (PC),37,39,40 cyclo-olefin copolymer (COC)39,41,42 and to a lesser extent PS.42 Several fabrication methods have been employed to produce thermoplastic microfluidic devices.[34] Of these methods, hot embossing is relatively simple and easy to implement, and has potential to become a cost-effective technique for producing microdevices in a laboratory setting in a manner that complements PDMS-based processes.

A major factor for the dominance of PDMS over thermoplastics in microfluidics research, particularly in academic laboratories, is the number of bottlenecks present in the process workflow for thermoplastic hot embossing microfabrication (Figure 1). First, PDMS allows a cost-effective optimization process that enables iterative design. Thermoplastic fabrication, in contrast, requires more expensive and labor-intensive processes, which include creation of micro-machined molds that require polishing to achieve high quality surface finishes. This may be acceptable in a commercial setting once a design has been finalized, but becomes

costly for research laboratories involved in early stages of design and development. Second, after a design is chosen, PDMS offers a rapid, repeatable process for generating a sufficient supply of devices for laboratory use. Whereas PDMS can be readily bonded to glass, plastics, and to itself via plasma treatment or other methods, monolithic devices made entirely of thermoplastics must rely on more challenging techniques such as thermal bonding, or those that involve adhesives, solvents, or ultrasonics that have been adopted much less frequently than plasma-assisted bonding.[34] To facilitate the use of PS for microfluidic cell biology applications as an alternative material to PDMS, it is necessary to establish a process that is accessible, affordable, efficient, and reliable, at a level competitive with soft lithography. Doing so will allow biologists to more easily adopt thermoplastic devices in their research and to take advantage of relevant microscale phenomena without being concerned about the adverse effects of PDMS.

In this study, we present a streamlined PS microfabrication process for creating arrayed microfluidic cell-based platforms, with the primary goal of establishing a set of protocols that are similar in reliability, and in cost and time expenditure compared to the PDMS-based soft lithography process. We hope to provide an alternative fabrication methodology that gives researchers working at the interface between microfluidics and biology a material consistent with existing laboratory cultureware. To achieve this, we (1) optimized the fabrication of inexpensive solid epoxy molds that used the same equipment as traditional SU-8 master fabrication; (2) developed a novel method to quickly generate arrays of access ports via a through-hole embossing technique that eliminates laborious drilling or punching procedures; and (3) optimized and characterized a thermal diffusion bonding process to bond PS sheets and films over large areas (100 × 100 mm) and with sufficient strength to withstand long-term cell culture applications in humidified environments. For clarity in nomenclature, we refer to each bonded PS sample as a *device* consisting of an *array of microsystems*. Each microsystem in the array represents an independent experimental condition, and may consist of network(s) of *microchannels*.

Experimental Section

Epoxy Mold Fabrication

The first two steps in our process were equivalent to those for the soft lithography process currently used in many microfluidics laboratories,[1,43] namely (1) the design and printing of photomasks, and (2) the fabrication of a master mold using SU-8 photoresist (Microchem, Newton, MA, USA). Briefly, SU-8 photoresist was spincoated on a silicon wafer (WRS Materials, San Jose, CA, USA) to the desired film thickness, pre-baked, exposed to UV light (EXFO, Mississauga, Canada), post-baked, and finally developed in propylene glycol monomethyl ether acetate (PG-MEA, Sigma, St. Louis, MO, USA). Draft angles on tall features were obtained by aligning the UV light-guide at an angle of 30–35 degrees from normal, and manually rotating the wafer on a turning plate during exposure. Doses were doubled to account for the angled exposure and the rotation.

A negative mold of uniform thickness was made in PDMS (Dow Corning, Midland, MI, USA) from the SU-8 master using typical curing parameters (10:1 mixing ratio of elastomer base and curing agent, 90°C, 1 h) (Figure 2A). Uniformity of the layer thickness was critical, and was achieved by laying a large glass slide on top of two 2.5-mm thick spacers. The PDMS slab was gently demolded from the wafer without detaching from the large glass slide, thereby preventing shrinkage of the features. A 15-mm tall PDMS ring was laid around the features to form a cavity into which a thermocurable epoxy (EC-415, see Materials and Preparation) was poured and allowed to fill the negative-relief features of the PDMS mold (Figure 2B). Air bubbles trapped in the mold features were dislodged manually with a sharp tool. Desiccating the PDMS mold prior to pouring the epoxy reduced the

incidence of these bubbles. Following manufacturer's specifications, the epoxy was cured for 24 h on a 40°C hot plate, followed by a four-stage heat treatment (93°C for 2 h; 121°C for 2 h; 149°C for 2 h; 177°C for 2 h) in an oven, and subsequent cooling to ~60°C before removing from the oven. The result was a solid positive-relief epoxy mold that replicated the original SU-8 master (Figure 2C).

Materials and Preparation

PS raw materials were purchased from Goodfellow (Cambridge, MA, USA) in various stock thicknesses, including 1.2 mm-thick stock sheets (#ST313120, amorphous), as well as 50, 125, and 250 μm-thick stock films (#ST311050, ST311125, ST311250, respectively; biaxially oriented). Thick stock sheets can be pre-cut to size using a razor blade or a laser cutting machine (Jinan Artsign Ltd., Jinan City, China) (not required), whereas thinner stock films can be cut to size with scissors. After cutting, PS sample pieces were either used as is, at 1.2 mm thickness, or flattened to other desired thicknesses using a hydraulic heated press (see Hot Embossing). The PS sample was placed between two mirror-finished stainless steel plates (McMaster-Carr, Elmhurst, IL, USA) to ensure optical transparency. Two metal shims (feeler gauge set, Grainger, Chicago, IL, USA) were used as spacers on opposite sides of the PS part to ensure uniform desired thickness (Figure 2D). Parameters used in the PS flattening protocol are listed as part of Figure 2G. As an alternative method to flattening PS sheets, desired thicknesses were also attained by stacking the appropriate PS films together, e.g., a 475 μm-thick PS layer could be achieved by stacking one 250-μm, one 125-μm, and two 50-μm layers together.

Cyclo-olefin polymer (COP) sheets were purchased from Ajedium Films (Ajedium, Solvay Solexis Inc., Newark, DE, USA) as 610-μm thick sheets made from Zeonor COP (1420R grade).

We tested three different epoxies to determine the material most suitable for our applications and our processing requirements: (1) Conapoxy FR-1080 (Cytec Industries Inc., Olean, NY, USA); (2) RenCast 4037 (Freeman Manufacturing, Avon, OH, USA); and (3) EC-415 (Adtech Plastic Systems, Madison Heights, MI, USA).

Hot Embossing

Hot embossing was carried out using a programmable 15-ton hydraulic press with heated platens (Model #3889, Carver Press, Wabash, IN, USA). Two different approaches were used for embossing microfeatures into PS, the choice of which was dependent on the nature of the features. The first approach embossed the pattern into the PS without penetrating the material (i.e., the non-through-hole embossing approach). In this approach, the hydraulic press platens were first heated to an initial temperature of 125°C, ~25°C above the glass transition temperature of PS. The PS sample was then loaded into the press in an arranged stack consisting of (from bottom to top): (1) a mirror-finished stainless steel plate; (2) PS sample; (3) epoxy mold; (4) 1-mm thick silicone rubber (McMaster-Carr, Elmhurst, IL, USA); and (5) ~380-μm thick Teflon film (McMaster-Carr, Elmhurst, IL, USA) (Figure 2E). After loading, the press was closed with an applied force of 900 kgf (2000 lbs) for 15 min (Figure 2G, non-through-hole emboss). An in-house cooling system, consisting of a water chiller (Model #ER301, Elkay, Oak Brook, IL, USA; available from McMaster-Carr) and water pump, was connected via tubing to the platens of the hydraulic heated press in order to accelerate the cooling step in the recipe. Once cooled to ~70°C, the press was opened, and the PS sample was carefully demolded from the epoxy mold.

The second approach was used to emboss the pattern into the PS with penetration of the material at specific locations (i.e., the through-hole embossing approach). With respect to

microsystem designs, through-holes are needed as access ports to the microsystem pattern. In this approach, the platens were first heated to 135°C prior to loading the arranged stack containing the PS sample. The arranged stack was similar to the non-through-hole approach, but consisted of an additional 610-μm thick COP sheet and a cellulose acetate film (Cheap Joe's, Boone, NC, USA) between the stainless steel plate and the PS sample. An automated embossing recipe (Figure 2G, through-hole emboss) was applied to the stack using the hydraulic press. Cooling and demolding steps were similar to the non-through-hole approach. Note that although PS is able to reflow at these temperatures, the sample needed to be thinner than the height of the tallest mold features by ~100 μm to achieve complete penetration of the mold.

Thermal Bonding of PS Devices

To form enclosed PS devices, thermal diffusion bonding was applied to top and bottom PS sample pieces. Depending on the design, the bottom PS sample was either a simple flat sheet without features (plain substrate), or a PS layer consisting of embossed features; the top PS part was a PS layer containing microchannels and through-hole access ports. In both cases, the top and bottom PS samples were blow-dried with compressed air, and arranged in a stack consisting of (from bottom to top): (1) stainless steel plate; (2) bottom PS layer; (3) top PS layer; (4) COP sheet; (5) silicone rubber; and (6) Teflon film. The hydraulic press was pre-heated to 90°C for 10 min after which the stack was loaded and the press closed with the required force and for the required time (Figure 2F). The platens were cooled to ~70°C before the bonded PS device was removed from the press. Different applied forces and bonding times were tested to determine optimal bonding parameters (see Bond Strength Characterization). In separate experiments, thermal bonding was also tested after applying sonication (10 min, 50°C) and oxygen plasma treatment (30 sccm, 60 W, 12 seconds) on the PS samples.

Bond Strength Characterization

Bond strength was quantified using a crack propagation method and surface energy calculation as an approximation.[44] Briefly, a 50-μm thick metal shim was inserted between two bonded PS layers, resulting in delamination of the bonded pieces in the form of a propagating crack line. The inserted shim and crack region were imaged together on an Olympus SZX16 stereoscope (Olympus, Center Valley, PA, USA), and the delamination length (i.e., average distance between inserted shim and propagation crack line) was measured using ImageJ software (NIH) (Figure 3C). Shorter delamination lengths corresponded to higher surface bond energies, referred to as bond strength [J/m^2] hereafter. We tested a minimum of three independently bonded devices ($n \geq 3$) for nine different sets of bonding parameters (900-kgf, 1350-kgf, and 1800-kgf applied force, each at 15, 30, and 60 min, with no surface treatment) to determine trends associated with force and time. From these data, one set of parameters was chosen (1350-kgf applied force, 30 min) for further analysis of bond strength with different surface treatments (sonication and oxygen plasma).

Cross-section Analysis

Cross-section analysis was performed on three representative sets of bonding parameters to illustrate how bonding parameters affected cross-sectional shape of microchannels. Bonded devices were cut near the desired cross-sectional plane on a VC-50 precision diamond saw (Leco, St. Joseph, MI, USA). The cut samples were wet-sanded to a glossy finish using 800- and 1200-grit sandpaper, respectively. After achieving the desired finish, the sectioned sample was sonicated in deionized water (10 min, 60°C) and dried. Imaging was performed on an Olympus SZX16 stereoscope.

Evaluation of Device Functionality

Bond quality and microchannel cross-sectional deformation were further evaluated by testing whether fluid flow was blocked in microchannels after thermal bonding. We designed a microsystem containing microchannels of three different (width-to-height) aspect ratios (AR = 10, 20 and 50), all with the same height of 10 μm. Twelve microsystems were placed in a 3 × 4 array on a single 50 × 75 mm device and fabricated using the through-hole embossing method. The device was then bonded using five of the nine sets of bonding parameters tested for bond strength: (1) 900-kgf, 15 min; (2) 900-kgf, 60 min; (3) 1350-kgf, 30 min; (4) 1800-kgf, 15 min, and (5) 1800-kgf, 60 min. Tests were conducted by flowing colored dye into each microchannel on the device, and counting the number of blocked microchannels.

Cell-based Applications

For our first application, arrays of straight microchannels (150 μm high, 1.5 mm wide, 22 mm long, 1 × 6 array) were fabricated by bonding a through-hole embossed port layer with a non-through-hole embossed microchannel layer, resulting in straight channels containing three access ports. Human umbilical vein endothelial cells (HUVECs) were cultured in EBM-2 media containing SingleQuots (Lonza, Allendale, NJ, USA), and seeded into the microchannels at 3,000 cells/μL. HUVECs were then cultured to confluence over 48 hours, and treated with 10 ng/mL IL-1β for 4 h to induce E-selectin upregulation.[45] After 4 h, HUVECs were fixed, permeabilized and immunostained with monoclonal anti-human E-selectin antibody (R&D Systems Inc., Minneapolis, MN, USA) and Hoechst 33342, nuclear dye (H1399, Invitrogen, Carlsbad, CA, USA). Images of the culture were acquired on a Nikon Eclipse Ti inverted fluorescence microscope (Nikon Instruments, Melville, NY, USA).

For our second application, a microfluidic chemotaxis system (described in detail elsewhere46) was fabricated in PS from a 700-μm through-hole embossed layer and a 125-μm sheet for the bottom. The top layer was treated in oxygen plasma for 50 seconds at 100 W prior to bonding, and the bottom layer was left untreated (i.e., one-side plasma treatment). 5 μL of fibronectin at 50 μg/mL was used to fill the microsystem by capillary action. After 1 h the device was rinsed with 5 μL of EBM-2 media with SingleQuots (see above). We purified peripheral blood neutrophils from human blood using Polymorphprep according to the manufacturer's recommendations (Nycomed, Sheldon, UK). All donors were self-reportedly healthy, and we obtained informed consent at the time of the blood draw. The human subject protocol was approved by the University of Wisconsin Center for Health Sciences Human Subjects Committee. The cell suspension was diluted to 500 cells/μL. 3 μL of the neutrophil suspension were loaded into one side of the microsystem, and 2 μL of chemoattractant (fMLP) was added to the other side. Time-lapse phase contrast optical microscopy was performed at 10× magnification by taking one frame every 30 seconds using an Olympus IX81 microscope. Tracking of neutrophil migration was performed using software developed in-house (available upon request).

Results and Discussion

Cell-based applications have specific challenges that can prevent current microfabrication processes from becoming widely adopted in a research context. Because cells are regulated by a complex set of soluble signals, mechanical stimuli, and other microenvironmental cues,[33] a large number of variables need to be investigated and controlled to properly explore such large parameter spaces.[47] The ability to fabricate arrays of microsystems is therefore an important step in enabling high-throughput microfluidic cell-based studies. We were able to achieve this through the optimization of a streamlined method for fabricating robust and

inexpensive epoxy molds from existing SU-8 masters, which enabled a through-hole embossing technique for PS that obviated the need for manual drilling or punching of ports. The protocols were also tailored to be simple and functional for use with affordable benchtop heated presses. Thus, with this relatively accessible and cost-effective method, rapid prototyping of arrayed microsystems in PS - and potentially other thermoplastics – can be achieved with cost and time expenditures approaching that of PDMS-based fabrication (Figure 1).

The fabrication methods developed here are compatible with a wide range of microfluidic designs, functionalities and pumping schemes. The ability to emboss through-hole ports directly makes the presented methods particularly well suited for operation by passive pumping.[48] This pumping scheme can be performed using common micropipettes and has been shown to be well suited for creating accessible cell-based assays. Certain design considerations, however, are critical for successful fabrication of functional and reliable devices. We discuss below important aspects of the fabrication process, from creating epoxy molds for hot embossing to bonding devices and preparing microsystems for culturing cells, in order to facilitate better translation to other applications.

Mold Design

A well-designed mold is critical to a successful embossing procedure because it can impact mold longevity, fidelity in replication of the features, and quality of the bond in the final device. The designer should consider several geometric mold parameters, including its overall size, draft angle of the features, and feature aspect ratios. First, larger mold sizes tend to reduce the uniformity of the embossing and bonding of the PS parts, resulting in a less reliable fabrication process. This non-uniformity, caused by minor misalignment of the press platens, can be partially compensated by the use of a layer of firm silicone foam rubber to equilibrate pressures across the sample. The protocols described here used a 50 × 75 mm epoxy mold; we have also achieved devices using molds up to 100 × 100 mm on the same hydraulic press by adjusting the applied force accordingly (Figure 4).

Second, demolding of the embossed part must be done carefully to preserve a high-quality part, and this can be assisted by proper inclusion of draft angles on all mold features. We found that features less than 50 μm tall generally do not require a draft angle, whereas a draft angle is critical for taller features such as through-hole access ports. A draft angle of 15 degrees typically produced good results for parts embossed with CNC (Computer Numerical Control) machined aluminium molds. To achieve a draft angle on our epoxy molds, we used an angled UV exposure technique to create angled side walls on SU-8 masters (Figure 3A). Note that the design of the features in the microsystem must account for the draft angle, which will increase the base-width of features.

Epoxy Mold

Hot embossing of PS requires molds that can withstand temperatures of 135°C (or higher for other thermoplastics) while under high pressures. Traditionally, these molds are fabricated by CNC machining of aluminum or steel, which involves fabrication and polishing steps that are both time consuming and costly. Silicon-SU-8 molds cannot be used directly for embossing since layered features are prone to delamination during the demolding step. To overcome this limitation, Mehta and co-workers developed a method to fabricate bulk epoxy molds (which were not susceptible to delamination) from regular silicon SU-8 molds.[42] While the concept was an important step in improving the process, we found that the choice of epoxy type was critical to mold strength and longevity because the operating pressures and temperatures we used in our processes were at the working limit of most epoxy materials. We tested three different epoxies, including Conapoxy, RenCast, and EC-415, to

observe their deformation after the embossing process. RenCast and EC-415, both aluminum-filled composite materials, showed little deformation, whereas Conapoxy (used by Mehta and co-workers) deformed significantly and produced molds whose features became distorted after one embossing cycle. EC-415 ultimately proved to be the most stable over multiple embossing cycles and allowed the fabrication of 15 to 20 parts with through-holes (more parts are possible without through-holes) before displaying excessive deformation. Our process permits easy fabrication of additional epoxy molds from the PDMS master mold. Importantly, the material strength of EC-415 enabled embossing of through-holes in the PS parts, which was particularly demanding for molds because of the need for higher embossing pressures. To assess mold longevity, the deformation of a mold used for through-hole embossing was monitored over a series of hot embossing cycles (Figure 3B). Results showed that the first emboss led to the largest change in port height; subsequent embosses resulted in relatively smaller changes at a constant rate. For the mold used in the experiment, in which the tallest features measured 700 μm, a deformation of ~10% resulted after 15 cycles. In addition, since the epoxy precisely replicates the original SU-8 master, the microfluidic channels displayed excellent optical transparency, and bonding surfaces were smooth. In comparison, aluminum CNC machined molds required an expensive and labor-intensive polishing step before they could be used for fabrication of channels with sufficient optical transparency to produce quality microscope images from cell-based studies.

Hot Embossing

Hot embossing relies on the viscoelastic properties of thermoplastic materials that are above its critical glass transition temperature (T_g), which is approximately 95 to 100°C for PS.[49] Embossing temperatures of 125°C and 135°C were chosen for non-through hole and through hole embossing, respectively, as it provided a good compromise between preservation of the epoxy mold and melt flow of the polymer.[50,51] In addition, to prevent the formation of sink marks in the embossed PS layer,[52] it was necessary to maintain constant applied force at the end of the last dwell step, until cooling of the press to a temperature of 75°C or less. For the more straightforward case of non-through-hole embossing, 125°C for 15 min was generally sufficient to produce good replication of features up to 1.2 mm in height.

In the more complex process of through-hole embossing, a higher temperature was preferable to prevent the formation of thin residual layers (i.e., membranes) in the regions where full mold penetration was desired. To facilitate the complete penetration of the mold through the PS layer, a sacrificial polymer backing layer was added. This material needed to be stiffer than PS at the dwell temperature, but soft enough to compress so that the epoxy mold was preserved. For convenience, COP with a T_g of 136°C was chosen because its T_g was higher than the range of temperatures compatible with PS embossing. Furthermore, the thickness of the PS sheet used for the embossing needed to be ~100 μm thinner than the height of the tallest port features of the mold. To prevent stiction between COC and PS, a thin cellulose acetate (CA) film was placed between them. This multilayer molding approach has been used previously for molding poly(oxymethylene) (POM), with CA as the backing polymer layer, and worked well because of the extremely low T_g of POM (T_g ~ negative 30°C).[52] The use of multilayer molding for through-hole embossing of PS has not been previously reported. This was an important technical achievement in our process because it provided a reliable and repeatable method for direct embossing of access ports in arrays of microsystems, which in some cases can contain hundreds of ports. Thus, this technique removed a bottleneck in the fabrication process by obviating the need for conventional drilling or punching operations for creating access ports.

Thermal Diffusion Bonding of PS

For applications in cell biology, solvent bonding methods were discounted because of the potentially harmful effects of bonding solvents (e.g., acetonitrile, toluene) on live cells in culture. Thus, we opted for thermal bonding as a chemical-free method for our cell-based devices. While others have previously demonstrated thermal bonding of PS microchannels for cell-based applications,[53] it was necessary for us to extend this work to achieve high bond quality over large arrays of microsystems. Since it has been suggested that thermal bonding below T_g can minimize channel deformation,[54] we focused on a low temperature bonding process to reduce variations in channel dimensions that may subsequently affect surface area-to-volume ratios that are critical in cell biology studies,[55] and ultimately bias biological readouts. To find an optimal bonding recipe, we explored different bonding times and pressures, and then measured bond strength and evaluated bond quality by examining channel deformations.

For bonding temperature, 90°C was chosen because it was high enough to permit thermal diffusion bonding but below the T_g of PS. We found that this temperature provided good bonding of the entire device surface over a range of dwell times and pressures, allowing the bonding process to be readily adjustable. Lower forces and times (1350 kgf for 30 min) displayed little deformation when we examined channel cross-sections, while higher forces and longer times (1800 kgf for 60 min) showed significant deformation (Figure 3C). We quantified bond strength for different values of the applied force (900, 1350, and 1800 kgf) and the dwell time (15, 30, and 60 min) using a crack propagation method that determined bond surface energy (Figure 3D).[44] Results for 900 and 1350 kgf showed expected trends where increasing the time led to increased bond strength. Also, for all bonding times, increasing the applied force led to higher bond strength, although results for 1800 kgf were inconclusive due to high variability in the results (Figure 3E).

We designed an indirect method to quantify, over a whole array, the level of deformation of the channel ceiling as a function of channel aspect ratio. An array of 24 microsystems was fabricated, each containing a set of microchannels of (width-to-height) aspect ratios of 10, 20, and 50. Five different bonding recipes were tested for channel ceiling collapse by determining whether colored dye was able to flow into the microchannel (Figure 3F). Results showed that bonding for longer times (60 min) led to more collapse of the channels and therefore less reliability in the effective channel heights. Of all the recipes tested, 1350 kgf (3000 lbf) for 30 min appeared to provide the best bond strength with highest aspect ratio achievable without failure (AR = 20), and therefore, was the optimal bonding protocol for our devices (the recommended bonding recipe in Figure 2G). Furthermore, this set of results suggested that maximum variability in channel height over the whole array is 5% (1/20 of the channel width). This was an important assessment of device reliability for cell-based assays because of the importance of consistency in channel dimensions for high-throughput applications.

Additional considerations for bonding can significantly improve bond quality and device functionality. A major difficulty when performing thermal diffusion bonding at low temperatures is ensuring good contact between the two surfaces. This difficulty is more apparent for larger device dimensions because sample unevenness is generally magnified for increased sizes. The use of a stiff and deformable polymer (COP) in combination with a foam layer improves local contact between the PS sheets without increasing deformation. Furthermore, bonding tests that used thinner PS sheets (250-μm or 125-μm film on the bottom instead of 330 μm) provided further reductions in deformation for the same recipe. Using thinner bottom PS layers is also advantageous from a practical perspective because it allows high-resolution imaging (with 40× objectives or higher magnification) for live studies of intracellular dynamics and other applications.

Surface Treatment

An important aspect for creating devices suitable for cell-based applications is the ability to modify the substrate surface to enable cell adhesion and growth while also preventing bubble formation. In the case of existing tissue culture plasticware, surfaces are rendered hydrophilic by exposure to low-powered oxygen plasma.[56] Several methods can be employed to achieve the same effect in the PS devices described. For example, PS parts can be conveniently treated with oxygen plasma prior to bonding (e.g., neutrophil chemotaxis application discussed below). However, plasma treatment can impact bond strength by altering the chemical composition at the surface of the PS material.[57] Measurements of bond strength showed that treating the PS device with plasma significantly reduced bond strength compared to the untreated device (>100 fold for one-sided treatment and ~10-fold for two-sided treatment; Figure 3G). Generally, the bond strengths associated with one-sided plasma treatment were still sufficient for passive pumping-based applications even after 48 h in a cell culture incubator (37°C, 5% CO_2), particularly when PS parts were sonicated prior to bonding. If certain applications require higher bond strengths (i.e., those achievable by thermal bonding without plasma), alternative methods for creating surfaces amenable to cell culture are also conceivable. First, it is possible to protect the top surface with a masking layer, and perform plasma treatment after thermal bonding of untreated PS parts.[43] Second, microchannels can also be pre-coated with extracellular matrix proteins prior to cell seeding, in order to promote cell adhesion (see HUVECS culture application below).

Applications in Cell Biology

To demonstrate the flexibility of our process and its amenability to cell biology, we used our protocols to make various devices for different applications (Figure 5). First, a 1 × 6 array of straight channels was fabricated using a two-sided embossing process. These microchannels were used in validation experiments involving the upregulation of E-selectin in HUVEC monolayers activated by IL-1β. Results were as expected, i.e., IL-1β resulted in E-selectin expression above baseline levels (for no IL-1β treatment) (Figure 5A). The 48-h culture to reach HUVEC confluence (with feeding after 24 h) demonstrated that long-term cell culture was compatible with our fabrication methods and materials used. Second, a neutrophil chemotaxis device, previously developed in PDMS,[46] was fabricated as a 1 × 8 array in a single-sided embossing process using thin 125-μm PS film as a bottom bonding layer. After the addition of neutrophils and fMLP, the neutrophils migrated toward the source reservoir in a manner similar to that observed in PDMS-based devices (Figure 5B). This device, which included a 50-μm tall gradient channel, was more complex in geometry than the straight microchannel, and thus served as a good test for validating the fabrication process for small microchannels. Furthermore, because the devices were made using a 100 × 100 mm mold, it demonstrated that the process was extensible to larger molds and that the function of the channels could be preserved.

Conclusion

Protocols were developed to provide a streamlined methodology for the fabrication of PS devices of arrayed microsystems useful for a wide range of cell-based applications. While PDMS-based devices are appropriate for certain applications, the protocols provided here provide alternative solutions that exhibit comparable cost effectiveness and design-to-device turnaround times in relation to the soft lithography process. Additionally, we believe that several steps in our protocol solved a number of bottlenecks in the typical thermoplastic microfabrication process, rendering fabrication of large arrays of microsystems in PS and other thermoplastics amenable to increased adoption by biologists. Results demonstrate that large arrays of microsystems in PS can be easily fabricated for use in long-term cell studies. Nevertheless, while the methods developed here provide improvements at several key steps

in the fabrication process, some limitations remain, notably in the thermal bonding step where the potential for channel collapse increases when width-to-height aspect ratios are too high, and bond strength is reduced, but still sufficient for many applications, when plasma treatment is incorporated.

Acknowledgments

We acknowledge financial support from NIH-NCI (grant #CA137673) (D.J.B.), the Natural Sciences and Engineering Research Council of Canada (NSERC) postdoctoral fellowship (E.Y.), the Morgridge Institute for Research (MIR) doctoral scholarship (E.B.), and NHLBI (grant # R44-HL088785) (I.M.). D. J. B. has ownership interest in Bellbrook Labs LLC, which has licensed technology reported in this publication.

References

1. Duffy D, McDonald J, Schueller O, Whitesides G. Anal. Chem 1998;70:4974–4984.
2. Whitesides G, Ostuni E, Takayama S, Jiang X, Ingber D. Annu. Rev. Biomed. Eng 2001;3:335–373. [PubMed: 11447067]
3. Folch A, Toner M. Annu. Rev. Biomed. Eng 2000;2:227–256. [PubMed: 11701512]
4. Beebe DJ, Mensing G, Walker G. Annu. Rev. Biomed. Eng 2002;4:261–286. [PubMed: 12117759]
5. Ohno K, Tachikawa K, Manz A. Electrophoresis 2008;29:4443–4453. [PubMed: 19035399]
6. Moraes C, Wyss K, Brisson E, Keith BA, Sun Y, Simmons CA. Cell. Mol. Bioeng 2010;3:319–330.
7. Young EWK, Simmons CA. Lab Chip 2010;10:143–160. [PubMed: 20066241]
8. Yang CWT, Ouellet E, Lagally ET. Anal. Chem 2010;82:5408–5414. [PubMed: 20499853]
9. Oblak T, Root P, Spence D. Anal. Chem 2006;78:3193–3197. [PubMed: 16643013]
10. Genes L, Tolan N, Hulvey M, Martin R, Spence D. Lab Chip 2007;7:1256–1259. [PubMed: 17896007]
11. Young EWK, Wheeler AR, Simmons CA. Lab Chip 2007;7:1759–1766. [PubMed: 18030398]
12. Gomez-Sjoberg R, Leyrat A, Pirone D, Chen C, Quake S. Anal. Chem 2007;79:8557–8563. [PubMed: 17953452]
13. Ku C, Oblak T, Spence D. Anal. Chem 2008;80:7543–7548. [PubMed: 18729474]
14. Chung S, Sudo R, Mack P, Wan C, Vickerman V, Kamm R. Lab Chip 2009;9:269–275. [PubMed: 19107284]
15. Domenech M, Yu H, Warrick J, Badders N, Meyvantsson I, Alexander C, Beebe DJ. Integr. Biol 2009;1:267–274.
16. Young EWK, Watson MWL, Srigunapalan S, Wheeler AR, Simmons CA. Anal. Chem 2010;82:808–816. [PubMed: 20050596]
17. Huh D, Matthews BD, Mammoto A, Montoya-Zavala M, Hsin HY, Ingber DE. Science 2010;328:1662–1668. [PubMed: 20576885]
18. Tay S, Hughey JJ, Lee TK, Lipniacki T, Quake SR, Covert MW. Nature 2010;466 267-U149.
19. Moraes C, Chen J-H, Sun Y, Simmons CA. Lab Chip 2010;10:227–234. [PubMed: 20066251]
20. Eddington D, Puccinelli J, Beebe DJ. Sensor Actuat. B-Chem 2006;114:170–172.
21. Toepke M, Beebe DJ. Lab Chip 2006;6:1484–1486. [PubMed: 17203151]
22. Regehr KJ, Domenech M, Koepsel JT, Carver KC, Ellison-Zelski SJ, Murphy WL, Schuler LA, Alarid ET, Beebe DJ. Lab Chip 2009;9:2132–2139. [PubMed: 19606288]
23. Verneuil E, Buguin A, Silberzan P. Europhys. Lett 2004;68:412–418.
24. Heo Y, Cabrera L, Song J, Futai N, Tung Y, Smith G, Takayama S. Anal. Chem 2007;79:1126–1134. [PubMed: 17263345]
25. Discher D, Janmey P, Wang Y. Science 2005;310:1139–1143. [PubMed: 16293750]
26. Paguirigan A, Beebe DJ. Bioessays 2008;30:811–821. [PubMed: 18693260]
27. Paguirigan A, Beebe DJ. Integr. Biol 2009;1:182–195.
28. Meyvantsson I, Warrick J, Hayes S, Skoien A, Beebe DJ. Lab Chip 2008;8:717–724. [PubMed: 18432341]

29. Puccinelli J, Su X, Beebe DJ. J. Assoc. Lab. Automat 2010;15:25–32.
30. Barbulovic-Nad I, Yang H, Park P, Wheeler AR. Lab Chip 2008;8:519–526. [PubMed: 18369505]
31. Halpin ST, Spence DM. Anal. Chem 2010;82:7492–7497. [PubMed: 20681630]
32. Tolan NV, Meyer JA, Ku C-J, Karunarathne W, Spence DM. Pure Appl. Chem 2010;82:1623–1634.
33. Young EWK, Beebe DJ. Chem. Soc. Rev 2010;39:1036–1048. [PubMed: 20179823]
34. Becker H, Gaertner C. Anal. Bioanal. Chem 2008;390:89–111. [PubMed: 17989961]
35. Tsao C, DeVoe D. Microfluid. Nanofluid 2009;6:1–16.
36. Martynova L, Locascio L, Gaitan M, Kramer G, Christensen R, MacCrehan W. Anal. Chem 1997;69:4783–4789. [PubMed: 9406529]
37. Wabuyele M, Ford S, Stryjewski W, Barrow J, Soper S. Electrophoresis 2001;22:3939–3948. [PubMed: 11700724]
38. Brown L, Koerner T, Horton J, Oleschuk R. Lab Chip 2006;6:66–73. [PubMed: 16372071]
39. Greener J, Li W, Ren J, Voicu D, Pakharenko V, Tang T, Kumacheva E. Lab Chip 2010;10:522–524. [PubMed: 20126695]
40. Ogonczyk D, Wegrzyn J, Jankowski P, Dabrowski B, Garstecki P. Lab Chip 2010;10:1324–1327. [PubMed: 20445888]
41. Tsao CW, Hromada L, Liu J, Kumar P, DeVoe DL. Lab Chip 2007;7:499–505. [PubMed: 17389967]
42. Mehta G, Lee J, Cha W, Tung Y, Linderman J, Takayama S. Anal. Chem 2009;81:3714–3722. [PubMed: 19382754]
43. Jo B, Lerberghe LV, Motsegood K, Beebe DJ. J. Microelectromech. S 2000;9:76–81.
44. Maszara W, Goetz G, Caviglia A, Mckitterick J. J. Appl. Phys 1988;64:4943–4950.
45. Bevilacqua M, Stengelin S, Gimbrone M, Seed B. Science 1989;243:1160–1165. [PubMed: 2466335]
46. Berthier E, Surfus J, Verbsky J, Huttenlocher A, Beebe DJ. Integr. Biol 2010;2:630–638.
47. Warrick JW, Murphy WL, Beebe DJ. IEEE Rev. Biomed. Eng 2008;1:75–93. [PubMed: 20190880]
48. Berthier E, Beebe DJ. Lab Chip 2007;7:1475–1478. [PubMed: 17960274]
49. Powell, PC.; Housz, AJI. Engineering with polymers. Cheltenham, UK: Stanley Thornes (Publishers) Ltd.; 1998.
50. Knoff W, Hopkins I, Tobolsky A. Macromolecules 1971;4:750–754.
51. Narkis M, Hopkins I, Tobolsky A. Polym. Eng. Sci 1970;10:66–69.
52. Worgull, M. Hot Embossing: Theory and Technology of Microreplication. Oxford, UK: William Andrew Publishers Elsevier Sci. Ltd; 2009.
53. Borenstein J, Tupper M, Mack P, Weinberg E, Khalil A, Hsiao J, García-Cardeña G. Biomed. Microdevices 2010;12:71–79. [PubMed: 19787455]
54. Bhattacharyya A, Klapperich CM. Lab Chip 2007;7:876–882. [PubMed: 17594007]
55. Walker G, Zeringue H, Beebe DJ. Lab Chip 2004;4:91–97. [PubMed: 15052346]
56. Barker S, LaRocca P. Method. Cell Sci 1994;16:151–153.
57. Grace J, Gerenser L. J. Disper. Sci. Technol 2003;24:305–341.

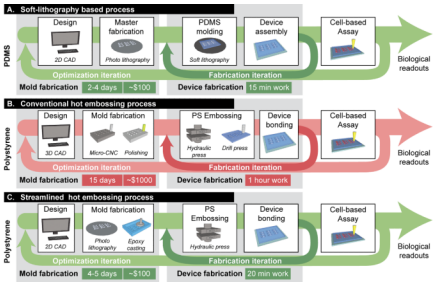

Figure 1.

Microfabrication process workflows: comparing PDMS to thermoplastics. (A) PDMS-based soft lithography process. Turnaround time from computer mask design to completed master mold is ~2–4 days. Costs include mask, wafer and SU-8 photoresist. (B) Current thermoplastic-based microfabrication process. ~10–15 days are required from design to usable mold; 1 hour is required for embossing, bonding and drilling access ports (for a platform containing 50–100 ports). Costs include mold machining and polishing. (C) Streamlined thermoplastic-based microfabrication process. Mold fabrication time is similar to (A) with an additional epoxy casting step. Costs are similar to (A) with the additional cost of the epoxy. Devices were fabricated more quickly using a through-hole embossing method that eliminated manual removal of access ports.

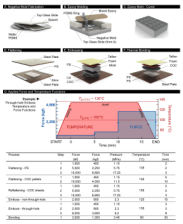

Figure 2.

Polystyrene microfabrication process. (A) Fabrication of a PDMS slab of uniform thickness to replicate the SU-8 master. (B) Casting of the epoxy in a PDMS cavity comprised of the replicate of the SU-8 mold and a PDMS ring. (C) Cured epoxy mold. (D) Flattening of PS sample to a desired thickness using metal shims. (E) Hot embossing of the PS sheet for through-hole fabrication (remove CA and COC for non-through hole approach). (F) Thermal bonding of two PS sample pieces. (G) Fabrication recipes for different hydraulic press procedures. Pressure is nominal value calculated based on mold surface area of 50 × 75 mm. Force-temperature functions used for through-hole embossing shown as example. Temperature curve consists of heating, dwell, and cooling phases. In the dwell phase, force may be successively ramped over time. During cooling, the final applied force during dwell was maintained to prevent sink marks in the embossed part.

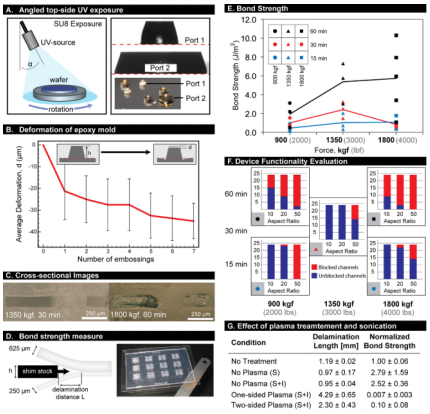

Figure 3.

(A) UV exposure for SU-8 features with draft angles. Collimated UV light is directed at an angle toward a SU-8-coated silicon wafer under rotation. After development, features display a profile with draft angles. (B) Deformation of the epoxy mold after repeated through-hole embossing. Largest deformation occurred after the first emboss. (C) Cross-sectional images for optimal bonding condition (1350 kgf, 30 min) and suboptimal condition (1800 kgf, 60 min) that led to significant channel deformation. (D) Schematic and image of bond strength test. (E) Bond strength results determined by crack propagation method. Total of nine conditions tested, all at least in triplicate (all data points shown to indicate data spread). (F) Evaluation of device functionality by counting number of blocked channels after bonding with given set of parameters. All 24 microchannels for each aspect ratio were measured (heights of bars), and categorized as blocked (red) or unblocked (blue). (G) Effect of sonication and oxygen plasma treatment on bond strength (values normalized to no treatment control). n = 3 for all conditions tested. Values represent average ± SD. S = sonication; I = incubation at 37°C, 5% CO_2.

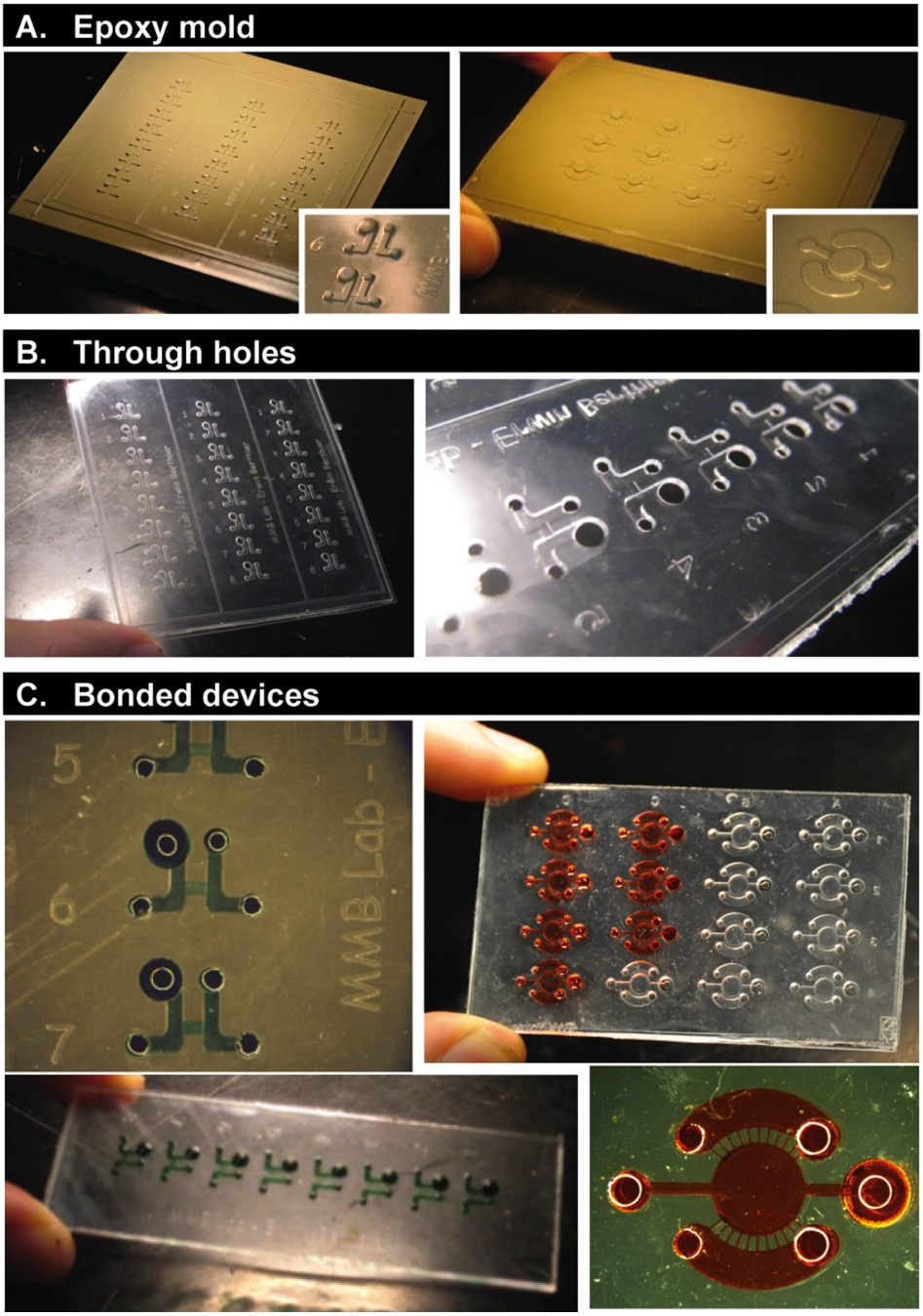

Figure 4.
Images of (A) epoxy molds, (B) through-hole embossed PS parts, and (C) bonded devices. The designs shown are for cell-based applications in neutrophil chemotaxis and non-adherent multiple myeloma cell immunostaining.

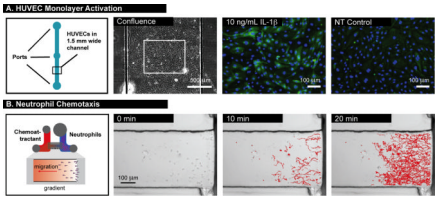

Figure 5.

(A) HUVEC monolayer culture and activation with IL-1β in a straight PS microchannel. E-selectin expression (green fluorescence) was upregulated after 10 ng/mL IL-1β treatment for 4 h. Nuclei were stained with Hoechst dye (blue). (B) Timelapse imaging and tracking of neutrophils migrating in a PS gradient device.